POLITECNICO DI MILANO
SCUOLA DI INGEGNERIA INDUSTRIALE E DELL'INFORMAZIONE

Master of Science in Automation and Control Engineering

Robust Harmonic Control for vibration suppression on helicopters

Name: Jose Luis Carratalá Broch
Supervisor: Prof. Marco Lovera
Co-supervisor: Prof. Roberto Mura

Academic Year: 2014-2015

A mi abuelo, reflejo de dedicación y esfuerzo .

Acknowledgements

I would like to acknowledge my family for the tremendous support they have given me through all this years of studies and also for the great opportunity they gave me because without them this wouldn't be possible. I am also grateful to my supervisor Prof. Marco Lovera and Co-supervisor Prof. Roberto Mura for the great work and all the support showed from the beginning.

Abstract

Helicopters have nice abilities like hovering and landing vertically thanks to the main rotor. Inherent to it there are important drawbacks related to noise and vibrations which make the helicopter inadequate to some situations and uncomfortable. With the purpose of reducing vibrations different technologies have been developed. In the case of this thesis High Harmonic Control (HHC) have been approached with an SISO overview of the LQ optimal control and a comparison between an structured and unstructured H_∞ robust control. The results showed faster response of the structured controller without great differences in terms of attenuation compared with the unstructured controller.

Contents

Chapter 1

Introduction

Abilities like taking off and landing vertically and hovering are nice features that give helicopters the center of attention in so many applications. However, one of the main problems affecting modern helicopters are the vibrations generated by the main rotor.These vibrations are caused by the non-uniform, unsteady rotor flow in forward flight as well as the interaction of rotor vortices with rotor blades for some flight conditions.Vibrations reduce the level of comfort of the pilot and passengers and increase the costs and maintenance efforts. Moreover high noise level becomes important in military missions and in public appearance such as EMS missions.

It is interesting to point out the frequency content of vibrations in the fuselage has an advantageous property. This means that whenever the rotor is well balanced, its dominating frequencies with N blades at a rotor rotational frequency Ω are:

$$\omega = mN\Omega \quad , m = 1, 2, 3...$$

and they are generated from NΩ and $(mN \pm 1)\Omega$ harmonics in the rotating frame. Regarding this, the rotor acts as a filter. The amplitudes usually become smaller with increasing frequency and rotors with more blades have less frequency content. In this way, using rotors with a larger number of blades seems to be a solution. However, this is normally not favourable since motor heads become more complex, expensive, heavier, etc.

Therefore, to reduce these drawbacks of helicopters, rotor control technologies have been investigated for a long time and, in this way, several approaches have been developed with this purpose.
These approaches fall into two separate categories: (a) passive control and (b) active control. At the beginning, when technology was not advanced enough, research focused on passive control technique. It is basically a system formed by spring and dampers, which acts on vibrations only after its generation, including generally a large weight penalty.They are simple, give a good stability and do not have power supply requirements but, their lack of adaptability to changes in

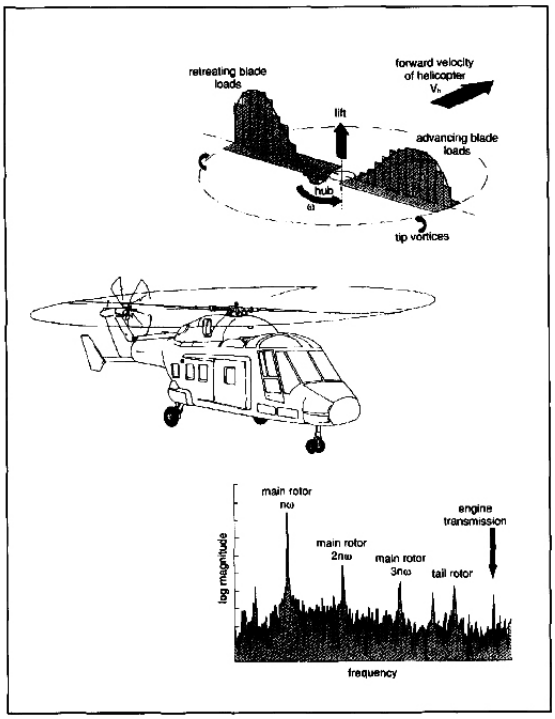

Figure 1.1: Helicopter fuselage vibration caused by rotor blade loads; ω =blade passing frequency, n =number of blades [11]

flight condition, rotor rotational frequency and changes in structural dynamics makes them less efficient.
As a result of advances in computing and actuating technology, active control approach was introduced in order to solve the problems related with passive control.These methods can offer a good vibration reduction, increasing comfort over significant areas of the aircraft structure and the main benefit of them is their capability to adapt to changing speed, rotor conditions and structural dynamics. Although the advantages compared to passive control, active control still presents problems related with external power source and its high complexity which makes the cost increase considerably. Figure 1.2 gives a layout of both technologies.

1.1 Target of the thesis

In the background of control theory, there have been many proposals over the years on how to implement active control for vibration reduction, but, little effort has been dedicated to the robustness problem of this kind of control system based on HHC. The aim of this study is to bring out a comparison between the optimal control and the robust control strategies. Specifically, exploring the HHC according to the LQ controller in the optimal control framework and using

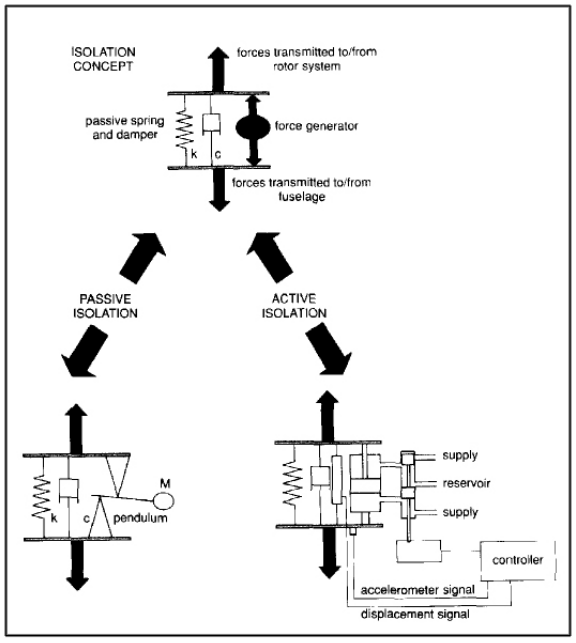

Figure 1.2: Passive and active isolation [11]

the H_∞ control in the robust controller point of view. Moreover, this work will examine the robust controller as a main alternative when including uncertainty due to changes in the flight condition and to the imprecise knowledge of the estimated T Matrix.

Chapter 2

State of Art

Early research on active control methods has motivated the development of different strategies to vibration reduction, but, the overall can be differentiated in two main categories: (a) active control approaches aimed to reduce vibrations before their propagation in the fuselage, and (b) active control approaches implemented directly in the fuselage using the so-called active control of structural response (ACSR). Inside the first category,Higher Harmonic Control (HHC) and Individual Blade Control (IBC) have emerged. Figure 2.1 illustrates this classification schematically.

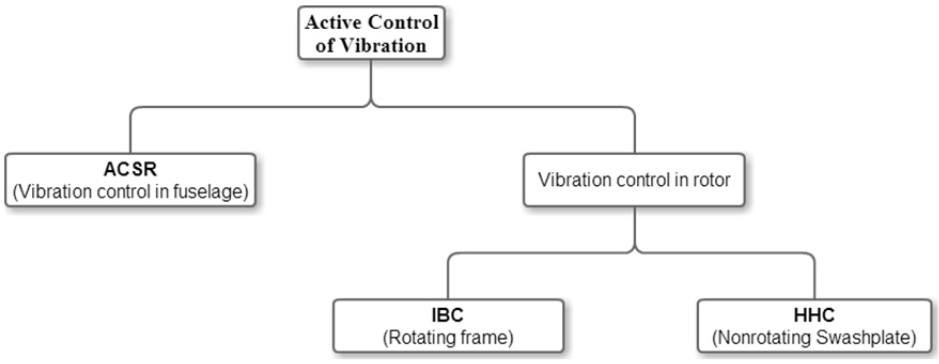

Figure 2.1: Classification of control approaches for Active Control of vibrations

These three alternatives are explained in the following:

Higher Harmonic Control (HHC)

It consists basically on the positioning of actuators below the swashplate in the non-rotating frame for rotors with more than three blades. This system operates creating blade oscillations in a way such that rotor head forces and moments are cancelled when properly phased. An important drawback of HHC is the limitation

to certain fixed control frequencies that depend on the number of blades NBl. The total blade pitch is given by the following:

$$\theta_i = \theta_0 + \theta_s \sin\psi_i + \theta_c \cos\psi_i + \theta_{HHC} \tag{2.1}$$

$$\theta_{HHC} = \theta_{n,HHC} + \cos(n\psi_i, \varphi_n) \tag{2.2}$$

$$\psi_i = \Omega t + \frac{2\pi}{N_{Bl}}(i-1) \quad , i = 1, 2, 3...N_{B1} \tag{2.3}$$

$$n = mN_{Bl}\, mN_{Bl} \pm 1; \quad m = 1, 2, 3... \tag{2.4}$$

where θ_i is the total blade pitch of the i-th blade θ_0, θ_s, and θ_c collective and cyclic inputs controlled by the pilot. θ_{HHC} is the HHC input which has three control variables: HHC amplitude $\theta_{n,HHC}$, HHC frequency $n\Omega$ and HHC phase ψ_n. The frequency factor n, unfortunately, is limited to integer multiples m of blade number mN_{Bl} and $mN_{Bl} \pm 1$.For instance a 4-bladed helicopter has a limitation to the following frequencies: 3,4,5/rev and integer multiples of the blade passage frequencies plus the next harmonics before and after it. Consequently the 2/rev frequency cannot be controlled for a helicopter with 4 blades. This frequency it is interesting to reduce noise or required rotor power as [6] reveals. Therefore, the more blades a helicopter has, the less frequencies can be controlled with HHC.

Individual Blade Control (IBC)

As said before, it is not possible to control the useful 2/rev frequency using HHC. This severe drawback, in addition to the not simultaneous reduction of noise and vibration, gave birth to an increasing research in Individual Blade Control. IBC is based on actuators in the rotation frame giving the opportunity to overcome these limits inherent to HHC.The differences between HHC and IBC have to be introduced. Inherent to HHC is a simpler design than IBC. It does not require transferring any electrical or hydraulic energy or signals from the fixed frame to the rotating frame. Furthermore the actuators are not exposed to centrifugal loads caused by the rotating rotor. However, IBC hydraulic actuators are mounted into the blades or in substitution to the push or pull rods between swashplate and pitch horn being affected by stress and torsion. There exist other two designs based on smart actuation technology by integrating either local or distributed piezo-ceramics into the blade. Further actuation concepts for IBC are being developed,but they remain out of the range of this paper.

IBC is understood in different ways depending on the author, but, generally, it can be defined as a system featuring as many control degrees-of-freedom as the rotor has blades no matter which type of actuation is used and no matter where sensors, power supply,etc. are integrated. IBC input is defined by some authors as:

$$\theta_{i,IBC} = \theta_n \cos(n\psi_i - \varphi_n)$$

where $\theta_{i,IBC}$ is the IBC blade pitch and ψ_i the azimuth of the i-th blade. The IBC input has three control variables: amplitude θ_n, harmonic number n and phase φ_n.

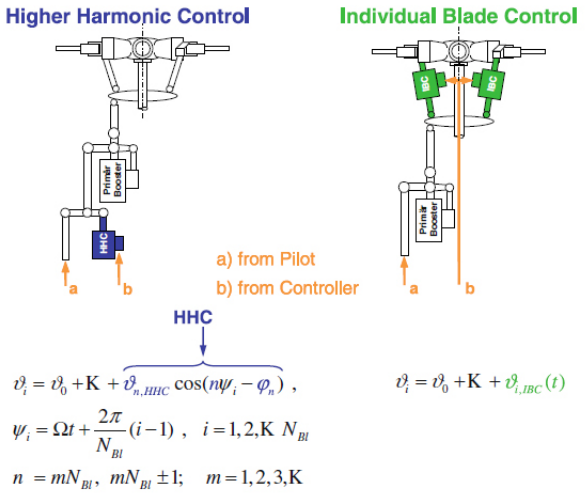

Figure 2.2: Comparison between HHC and IBC [12]

Active Control of Structural Response (ACSR)

The basic idea behind this control is to measure a number of points on the fuselage and the vibrations generated. This information is then processed by a multivariable control algorithm which calculates a set of control forces for a set of hydraulic actuators, located at strategic points in the structures. Vibration reductions results from the superposition of the actuator induced vibration forces with those induced in the fuselage by the rotor. The basic scheme is outlined in Figure 2.3

2.1 Evolution of HHC

First investigations on active rotor control technology based on HHC focused on the reduction of blade stall on the retreating side of the rotor disc by 2/rev control and a redistribution of the lift for increasing flight velocity by this control technique. Although first results were weak in terms of accuracy, a discussion was created around HHC, and research in this field began until today. After this first contact, two investigators focused on stall delay through HHC, and a first proposal for a mechanical HHC system arrived. The design included a curved track cut into the stationary part of the swashplates in Figure 2.4, with rotating control arms that ride in this track and move the push rods vertically. Still, the

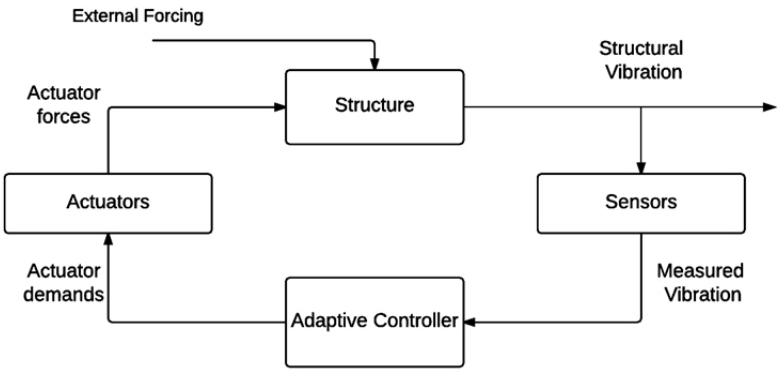

Figure 2.3: ACSR scheme

design suffered from significant drawbacks such as, the pre-shaping of the curved track, the impossibility of adapting HHC amplitude and phase to the flight state and the fact that the generated HHC input cannot be switch off, e.g. in hover.

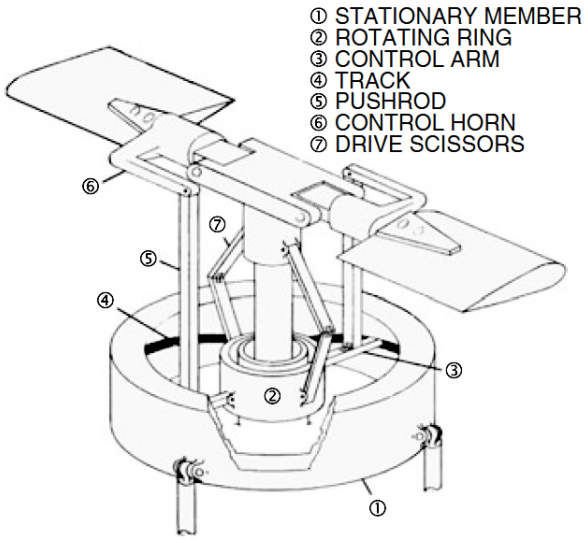

Figure 2.4: Mechanical HHC system [2]

Flight test were considered as not fully successful, but, the project did demonstrate the achievement of some reduction in vertical vibration by properly applying HHC. Some conclusions from this result were that the optimum phase angle depends on the target to be minimized and on airspeed. Therefore, beneficial effects of HHC on vibrations and load reduction ended up being relatively small, and, definitely, 2/rev HHC would not be effective in the delay of retreating stall. Hopefully, it turned out that these results may be different in the performance of other helicopters.

A second test flight was conducted by Hughes Helicopters, NASA and US army on an OH-6A, 4-bladed with an articulated rotor. The aim of this project was to reduce the 4/rev vibration component in the fuselage using a 3-5/rev HHC blade feathering. The test pointed out that a perfect amplitude of the HHC would result in an ellipse that crosses the origin and, therefore, it would cancel all normal force vibrations at the optimum phase. Manually, amplitude and phase were changed until optimal control parameters showed up to be amplitude 0.22^{o} and phase 30^{o} as seen in Figure 2.5.

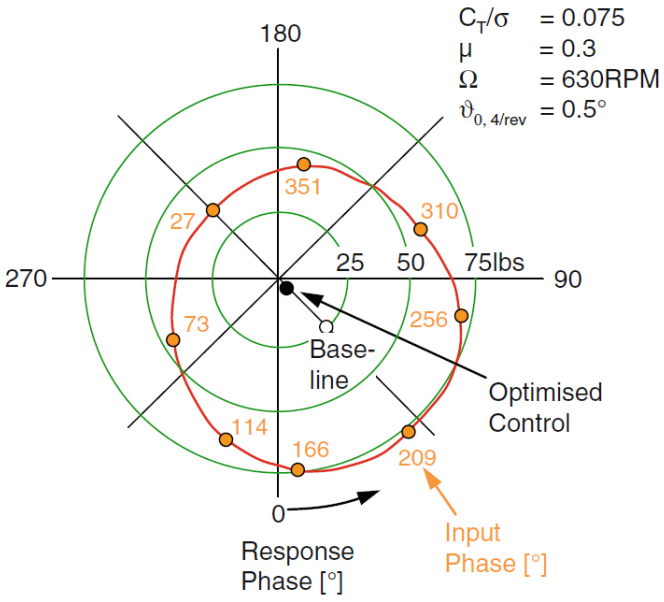

Figure 2.5: Variation of a 4/rev normal force of model rotor with 4/rev input [15]

Configurations do not eliminate all vibrations, but, resulting vibration reduction in normal phase is rather good. Moreover, it was also discovered that this optimized setting did have a negative impact on torsional moment, not in bending moments. After that, a second test was run applying HHC now in closed loop. It consisted in four different controller concepts based on Kalman filter algorithms. The purpose was the measurement of vertical force, pitching and rolling moment by a balance fixed to the rotor shaft. And, again, HHC could attenuate vibrations over a wide range of advanced ratios, but, it tended to follow same trajectory as former project: an increase in edgewise bending moment, torsional moment and control loads was discovered. Design of the mechanical HHC system was also updated and actuators in the nonrotating system replaced conventional rod-end links between the control mixer and the stationary swashplate.With this new configurations, test flights were performed in open loop and closed loop HHC, measuring vibrations at pilot's seat in all three directions. The algorithm used in order to control vibrations with the closed loop approach was based on the T

matrix approach.

$$Z_i = Z_{i0} + T_{ij}u_j$$

being Z_i the vector of measured vibrations composed by 3 sine and 3 cosine elements, Z_{i0} is the vector of the baseline vibrations levels to the HHC inputs and is the vector of HHC inputs (3-5/rev in sine and cosine). Such a purely linear relation would generate a perfect ellipse about the baseline condition in Figure 2.5. The estimation of the unknown parameters of the equation was obtained with a Kalman filter technique, while the estimation of the T-matrix requires an identification procedure. This initializes the process, possibly causing some annoying variations of the vibrations levels to pilot and passengers; however,this did not happen. Contrary to what was expected, control approach turned out to be very robust. As can be seen in the figure 2.6, vibrations can be reduced for vertical and lateral directions, but not for longitudinal; anyway, this is tolerable since longitudinal vibrations are rather small compared to vertical vibrations. The result is that vibration level decreases considerably.

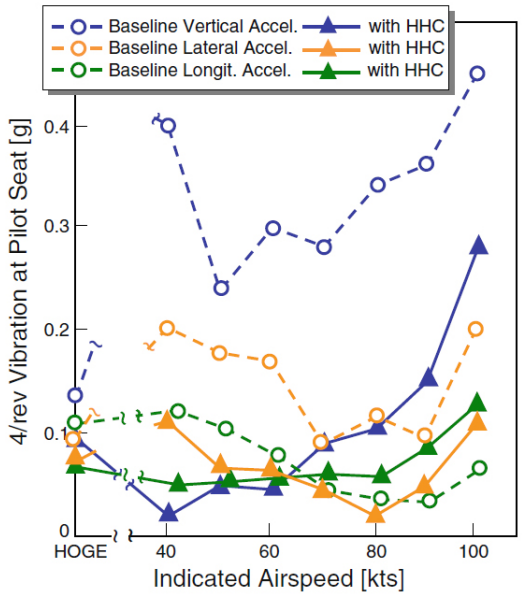

Figure 2.6: Pilot's seat vibrations with and without HHC in level flight [14]

After that, more wind tunnel test were computed with other rotor model [13]. Open loop tests confirmed an almost linear relation between vibrations and HHC inputs. However, since a strong impact of advanced ratio on HHC amplitude and phase was noted, conclusion was that T-matrix as a constant gain controller would not give satisfactory HHC performance.

30 years ago, more flight test based on T-matrix approach were computed by Aerospaziale on a SA349 Gazelle with 3-bladed articulated rotor. Now, the HHC system featured a closed loop self-adaptive controller. The achievement of

optimal HHC inputs was computed in three different ways, one of them by a preceding identification and the other ones by a permanent identification of the mentioned matrix. Different models and configurations were tested with one of the two adaptive configurations of the HHC, Figure 2.7 shows briefly the results, in which it can be noticed the improvement on vibration reduction that HHC could give.

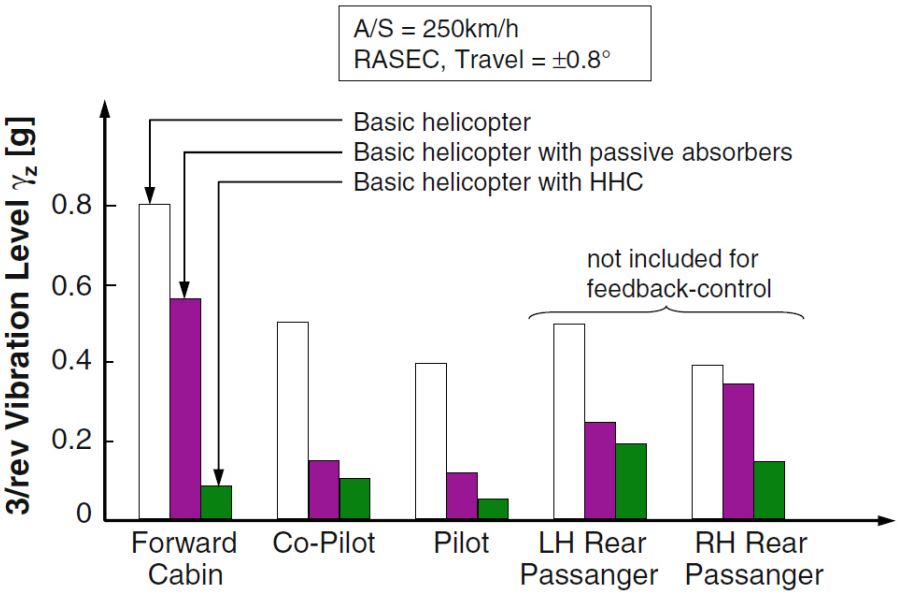

Figure 2.7: Comparison of vibration levels: Passive vs. Adaptive HHC [1]

At this point, it can be said that two ways of implementing HHC were opened for discussion, fixed-gain versus adaptive gain, from which adaptive approach was leading the field. Knowing that the initialization was not correct, the adaptive algorithm could rapidly react and adapt itself. Moreover, also in manoeuvring flights, this worked satisfactory. The fixed-gain controller was only effective for speed changes smaller than 20 kts.

Furthermore, international partners looking for this simultaneously reduction of noise and vibrations made a first HHC rotor aeroacoustic test in anechoic environment concluding, above all, that a significant reduction of vibration meant an increasing noise. So, the more beneficial parameters were for vibration reduction, the more noise increased, and vice versa. Configurations which gave a simultaneous reduction of vibrations and noise existed, but on expense of less attenuation of both parameters. Therefore, HHC lost popularity in the field, making IBC highly desirable.

Progress in technology of this field was translated in better highly instrumented test equipment. It supposed a great advance compared to the tests performed before. In this respect, two tunnel projects focused again on vibration and noise reduction, but, providing much more data than other campaigns were

Table 2.1: Test at constant amplitude (*) Much lower amplitudes are normally applied to reduce vibrations

3/rev control	Minimum Noise	Vibration Reduction*
Amplitud	0.85^{o}	0.85^{o}
Phase Angle	296^{o}	177^{o}
Simultaneous Reduction	2-3dB	-

able to deliver. First test presented huge differences; first of all, the model was restructured showing a slightly different steady and dynamic behaviour, moreover, microphones for acoustic radiation measurements and a wide variety of sensors were installed. There were found the minimum vibration and noise cases and also the minimum reduction of both simultaneously with the results shown in table 2.1

Important results were achieved by this test; above all, noise reduction mechanism should be remarked: increasing blade-vortex miss-distance was shown to be most important, followed by unloading the blade at the interaction, while vortex strength was found to be increased. The miss-distance itself was dominated by aerodynamically induced tip vortex convection rather than by blade flapping, i.e. the vortex draws aside the blade and not vice versa. So, consequently, the key parameter for noise stimulation is the wake simulation.Therefore the understanding of the mechanisms will support the design of robust control laws.

As explained before, last tests have been decisive for the better understanding of the behaviour of HHC. But, the main result is the interest that this better understanding could generate the proposal to the design of robust HHC control laws that would substitute the T matrix approach.

Chapter 3

Optimal control approach: LQ controller

3.1 Numerical Analysis

As seen in the previous section, HHC architecture has been formulated in many different ways over the years, and research has been focused mainly in it with the objective of the better understanding its behavior. It has been also pointed out that the first and main proposal for the algorithm was the T-matrix approach, which is a discrete, frequency domain technique that uses estimates of the disturbance on the previous cycles in order to cancel it during the current cycle. It basically defines the problem in the frequency domain and uses a LQ-like cost function in order to tune the controller.

The generalized T-matrix algorithm can be either implemented through a fixed-gain or an adaptive gain. This work will examine the fixed-gain approach.

3.1.1 The T-matrix Algorithm

Considering a SISO system, let u be the control input applied to the rotor and y the measured output; assume also that u is a piecewise periodic function of period $T = \frac{2\pi}{\Omega}$, where Ω is the rotor's angular frequency, let $\psi = \Omega t$, and define:

$$y_{Nc} = \frac{2}{T} \int_0^T y(\psi)\, cNd\psi \tag{3.1}$$

$$y_{Ns} = \frac{2}{T} \int_0^T y(\psi)\, sNd\psi \tag{3.2}$$

$$y_N = \begin{bmatrix} y_{Nc} \\ y_{Ns} \end{bmatrix} \tag{3.3}$$

and in the same way for u. Assume now that under steady state conditions the above defined N/rev harmonics of u and y are related by the linear equation:

$$y_N = T_{N,N} u_N + y_{0N} \tag{3.4}$$

where $T_{N,N}$ is a 2×2 constant coefficient matrix and the N/rev component of the "background" vibration that affect the system are indicated by y_{0N}. Since the dynamics of the controlled rotor can be assumed to be linear time-invariant, the matrix $T_{N,N}$ is, then, clearly related to the frequency response $G(j\omega)$ associated with the system by

$$T_{N,N} = \begin{bmatrix} Real(G(j\Omega N)) & Imag(G(j\Omega N)) \\ -Imag(G(j\Omega N)) & Real(G(j\Omega N)) \end{bmatrix} \tag{3.5}$$

In this way, the discrete time algorithm for the attenuation of the effect of y_{0N} on y known as the "T-matrix algorithm" is given by

$$u_N(k+1) = u_N(k) - T_{N,N}^{-1} y_N(k) \tag{3.6}$$

where k is the control cycle index. From this, it is easy to see from equations (3.4) and (3.6) that this control algorithm introduces a discrete-time integral action which ensures that $y_N \to 0$ as $k \to \infty$. Actually, if T matrix is exactly known it is possible to find out which input signal must be applied to the system so that the output achieves the steady-state condition in the smallest number of steps. This is known as deadbeat control.

Considering the problem, the objective is to answer the question of how actuators have to behave in order to attenuate the vibration disturbance; the system is the helicopter model of the coupled rotor-fuselage in the frequency domain; the control law refers to the way the actuators act, in other words, what will be the control input to be applied; and the optimality criterion is the minimization of the vibration disturbance.

From the optimal control viewpoint, the computation of the control law for the attenuation of the effects of the disturbance y_{0N} on y_N can be derived by minimizing at each discrete-time step k the LQ-like cost function. The LQ regulator is the tool which optimizes the control, specifying some kind of performance function to be optimized. In this way, the following is the cost function to be minimized:

$$J(k) = y_N^T(k) Q y_N(k) + 2 y_N^T S u_N(k) + u_N^T(k) R u_N(k) \tag{3.7}$$

where $Q = Q^T \geq 0$,$S = S^T > 0$ and $R = R^T > 0$. The control goal is to keep y_N as close as possible to 0. It can be noticed from the cost function that:

- $y_N^T(k) Q y_N(k)$ penalizes the transient state deviation, e.g. the weight on the parameters to be reduced, such as, the vibration levels.

- $2y_N^T(k)Su_N(k)$ penalizes the finite state.
- $u_N^T(k)Ru_N(k)$ penalizes the control effort, it is the weight on the control inputs.

Replacing k by $k+1$ in (3.4) and subtracting the resulting equation (3.4) itself, yields the disturbance-free update model

$$y_N(k+1) = y_N(k) + T_{N,N}(u_N(k+1) - u_N(k)) \tag{3.8}$$

Substituting now $y_N(k)$ from (3.4) into (3.7) brings in a new cost definition, namely

$$J(k) = u_N^T(k)Du_N(k) + 2u_N^T(k)T_{N,N}^T Qy_{0N}(k) + y_{0N}^T(k)Qy_{0N}^T(k) \tag{3.9}$$

where D is defined as:

$$D = T_{N,N}^T QT_{N,N} + R \tag{3.10}$$

Differentiating (3.9) with respect to $u_N(k)$

$$\frac{\partial J(k)}{\partial u_N(k)} = Du_N + 2T_{N,N}^T Qy_{0N}(k) \tag{3.11}$$

yields the control law:

$$u_N(k+1) = -D^{-1}(T_{N,N}^T Q)y_{0N}(k) \tag{3.12}$$

where

$$K_{N,N} = -D^{-1}(T_{N,N}^T Q) \tag{3.13}$$

As a matter-of-fact, the steps that the above algorithm follows are:

1. The determination of the N/rev component of y, namely the computation of the modulated integrals (3.1) and (3.2) of y.
2. The update of the N/rev component of u using equation (3.6) or equation (3.12)
3. The determination of the time domain value of the control input u via a modulation of the N/rev sine and cosine components.

It can be noticed that if the weight matrices Q and R are chosen as, respectively, the identity and zero matrices, then , the control law (3.12) reduces to (3.6); meaning that the optimization of the cost function, and, therefore, the best control input will be achieved in just one step, ideally.

The quality of the control tune using the LQ method depends on the choice of the weight matrices Q and R. The selection of them is basically computed by an

iteration procedure. By simulating the system, it can be analyzed the sensitivity to each weight function.

The control law can also be parameterized as

$$u_N(k+1) = K_M u_N(k) + K_N y_N(k) \tag{3.14}$$

where

$$K_M = -T_{N,N} K_{N,N} K_N = K_{N,N} \tag{3.15}$$

with $K_{N,N}$ given by (3.13). In this respect, it should be pointed out that the structure of matrix $T_{N,N}$ implies a similar structure of matrices K_M and K_N.Indeed, the matrices are not fully parametrized but are characterized by two independent parameters each, one for the diagonal and one for the off-diagonal ones (related to, respectively, the real and the imaginary parts of matrix $T_{N,N}$).

3.1.2 Convergence Analysis

A recursive form of the optimal control law is developed in Chandrasekar et al.(2004) in order to demonstrate the one-step convergence property. Substituting (3.12) into (3.7) and (3.4), the optimal value of y_k for all $k \geq 1$ is given by

$$y_{k,opt} = [I - T_{N,N} D^{-1} (T_{N,N}^T Q + S^T)](y_{0N} - T_{N,N} u_{0N}) \tag{3.16}$$

and thus

$$J(y_{k,opt}, u_{k,opt}) = (y_{0N} - T_{N,N} u_N)^T [Q - (QT_{N,N} + S) D^{-1} (T_{N,N}^T Q + S^T)](y_{0N} - T_{N,N} u_N) \tag{3.17}$$

These are the values that are attained after the first step update. Using equation (3.4), the optimal control law of equation (3.12) can be expressed recursively as

$$u_{k+1,opt} = -D^{-1}(T^T Q + S^T)(y_{k,opt} - T u_{k,opt}) \tag{3.18}$$

The state space representation of the system dynamics with the optimal control law is

$$\begin{bmatrix} y_{k+1,opt} \\ u_{k+1,opt} \end{bmatrix} = A \begin{bmatrix} y_{k,opt} \\ y_{k,opt} \end{bmatrix} \tag{3.19}$$

where A is a $2(p+m)x2(p+m)$ matrix defined by

$$A = \begin{bmatrix} I_{2p} - T_{N,N} K_{N,N} & -(I_{2p} - T_{N,N} K_{N,N}) T_{N,N} \\ -K_{N,N} & K_{N,N} T_{N,N} \end{bmatrix} \tag{3.20}$$

and

$$K_{N,N} = D^{-1}(T_{N,N}^T Q) + S^T \tag{3.21}$$

Note that

$$A^2 = \begin{bmatrix} (I_{2p} - T_{N,N} K_{N,N})^2 (I_{2p} - T_{N,N} K_{N,N}) T_{N,N} K_{N,N} & -(I_{2p} - T_{N,N} K_{N,N})^2 T_{N,N} - (I_{2p} - T_{N,N} K_{N,N}) T_{N,N} K_{N,N} T_{N,N} \\ -K_{N,N}(I_{2p} - T_{N,N} K_{N,N}) - K_{N,N} T_{N,N} K_{N,N} & K_{N,N}(I_{2p} - T_{N,N} K_{N,N}) T_{N,N} + (K_{N,N} T_{N,N})^2 \end{bmatrix} \tag{3.22}$$

$$= \begin{bmatrix} I_{2p} - T_{N,N}K_{N,N} & -(I_{2p} - T_{N,N}K_{N,N})T_{N,N} \\ -K_{N,N} & K_{N,N}T_{N,N} \end{bmatrix} = A \tag{3.23}$$

Hence, A is an idempotent matrix, e.g. $A^2 = A$, and its eigenvalues are either 0 or 1. To show this, note that A can be decomposed as

$$A = \begin{bmatrix} I_{2p} & T_{N,N} \\ 0 & I_{2m} \end{bmatrix} \begin{bmatrix} I_{2p} & 0 \\ -K_{N,N} & 0_{2m} \end{bmatrix} \begin{bmatrix} I_{2p} & -T_{N,N} \\ 0 & I_{2m} \end{bmatrix} \tag{3.24}$$

which implies that the spectral radius of A,

$$\max_{1 \leq i \leq n} |\lambda_i| = sprad(A) = \rho_s(A) \tag{3.25}$$

where A has n eigenvalues λ_i can be interpreted as the union of $\rho_s(I_{2p})$ and $\rho_s(0_{2m})$

$$\rho_s(A) = \rho_s(I_{2p}) \cup \rho_s(0_{2m}) \tag{3.26}$$

Recall that the eigenvalues of the identity matrix are $\lambda_{I_{2p}} = \{1, ..., 1\}$ and for the zero matrix $\lambda_{0_{2m}} = \{0, ..., 0\}$. Observing the block structure of the three matrices of equation (3.24), all the eigenvalues of the first and third matrix are 1, and the eigenvalues of the central matrix must be 0 or 1. With initial conditions y_{0N} and u_{0N} equation (3.19) implies that

$$\begin{bmatrix} y_{1,opt} \\ u_{1,opt} \end{bmatrix} = A \begin{bmatrix} y_{0N} \\ u_{0N} \end{bmatrix} \tag{3.27}$$

and

$$\begin{bmatrix} y_{2,opt} \\ u_{2,opt} \end{bmatrix} = \begin{bmatrix} y_{1,opt} \\ u_{1,opt} \end{bmatrix} = A^2 \begin{bmatrix} y_{0N} \\ u_{0N} \end{bmatrix} = A \begin{bmatrix} y_{0N} \\ u_{0N} \end{bmatrix} = \begin{bmatrix} y_{1,opt} \\ u_{1,opt} \end{bmatrix} \tag{3.28}$$

Similarly, for all $k = 1, 2, ...,$

$$\begin{bmatrix} y_{k,opt} \\ u_{k,opt} \end{bmatrix} = A \begin{bmatrix} y_{0N} \\ u_{0N} \end{bmatrix} = \begin{bmatrix} (I - T_{N,N}K_{N,N})(y_{0N} - T_{N,N}u_{0N}) \\ -K_{N,N}(y_{0N} - T_{N,N}u_N) \end{bmatrix} \tag{3.29}$$

This confirms the fact that optimum values $u_{k,opt}$ in equation (3.12) and $y_{k,opt}$ in equation (3.16) are attained after the first update.

3.1.3 Robustness of the T-matrix Algorithm

The main limitation of the T-matrix algorithm is that it relies on the exactly knowledge of the matrix, $T_{N,N}$ the control law (3.11) is based on the assumption that the $T_{N,N}$ matrix is available and known without error. However, in practical implementation this is not likely since changes in flight condition or non-linearities cannot ensure these assumptions. This drawback can lead to the implementation of an erroneous model and the performance can be degraded or even become unstable. In this way, a possible a posteriori analysis can be carried out in

order to prove robustness qualities. Focusing on the algorithm and taking into account the model (3.4) and the control law (3.14), one has that the problem to be investigated is the stability of the closed-loop system given by

$$\begin{aligned} u_N(k+1) &= K_M u_N(k) + K_M u_N(k) \\ y_N(k) &= T_{N,N} u_N(k) + y_{0N}(k) \end{aligned} \tag{3.30}$$

An interesting derivation is also implemented in Chandrasekar et. al(2004), where upper bounds on the maximum singular value of the additive uncertainty for which robust stability is guaranteed by using the above described LQ-control law. So, if $T_{N,N}$ is not known exactly, and only an estimate of $T_{N,N}$ is available, the control law by equation (3.18) becomes:

$$\widehat{u}_{k+1} = -\widehat{K}_{N,N}(y_k - \widehat{T}_{N,N}\widehat{u}_k) \tag{3.31}$$

where

$$\widehat{K}_{N,N} = \widehat{D}^{-1}(T_{N,N}^T Q + S^T) \tag{3.32}$$

In order to develop a condition for the stability of the algorithm of the algorithm, a state-space representation of the system-dynamics must be introduced, from equation)3.31),

$$\begin{bmatrix} y_{k+1} \\ \widehat{u}_{k+1} \end{bmatrix} = \widehat{A} \begin{bmatrix} y_k \\ \widehat{u}_k \end{bmatrix} \tag{3.33}$$

where $\widehat{A}$ is defined by

$$\widehat{A} = \begin{bmatrix} (I_{2p} - T_{N,N}\widehat{K}_{N,N}) & T_{N,N}(\widehat{K}_{N,N}\widehat{T}_{N,N} - I_{2p}) \\ -\widehat{K}_{N,N} & \widehat{K}_{N,N}\widehat{T}_{N,N} \end{bmatrix} \tag{3.34}$$

and $\Delta T = \widehat{T}_{N,N} - T_{N,N}$. It is useful to factor $\widehat{A}$ as

$$\widehat{A} = \begin{bmatrix} I_{2p} & T_{N,N} \\ 0 & I_{2m} \end{bmatrix} \begin{bmatrix} I_{2p} & 0 \\ -\widehat{K}_{N,N} & \widehat{K}_{N,N}\Delta T \end{bmatrix} \begin{bmatrix} I_{2p} & T_{N,N} \\ 0 & I_{2m} \end{bmatrix} \tag{3.35}$$

which shows that

$$\max_{1 \le i \le n} \left|(\lambda_{\widehat{A}})_i\right| = \rho_s(\widehat{A}) = \rho_s(I_{2p}) \cup \rho_s(\widehat{K}_{N,N}\Delta T) \tag{3.36}$$

Equation (3.36) yields insight on the stability of the system. Note that stability of the algorithm requires that the eigenvalues of $\widehat{K}_{N,N}\Delta T$ be such that:

$$\max_{1 \le i \le n} \left|(\lambda_{\widehat{K}_{N,N}}\Delta T)_i\right| = \rho_s(\widehat{K}_{N,N}\Delta T) < 1 \tag{3.37}$$

Neglecting cross-weighting term in equation (3.7), the cost-function is determined by

$$J(k) = y_N^T(k) Q y_N(k) + u_N^T(k) R u_N(k) \tag{3.38}$$

Therefore, considering equation (3.38), the spectral radius $\rho_s(\widehat{K}_{N,N}\Delta T)$ can be evaluated, if an operator σ_{max} is defined as the largest singular value of the matrix A

$$\sigma_{max} = \underset{1\leq i\leq n}{max} = (\sqrt{(\lambda_{A^*A})_i}) \tag{3.39}$$

where A^* in the adjoint or conjugate-transpose matrix of A, $A^* = (\overline{A})^T$. Similarly, an operator σ_{min} can be defined as the smallest singular value of matrix. Using these operators to expand the stability condition,

$$\begin{aligned}
\rho_s(\widehat{K}_{N,N}\Delta T) &= \rho_s((\widehat{T}_{N,N}^T Q\widehat{T}_{N,N} + R)^{-1}\widehat{T}_{N,N}^T Q\Delta T) \\
&\leq \sigma_{max}((\widehat{T}_{N,N}^T Q\widehat{T}_{N,N} + R)^{-1}\widehat{T}_{N,N}^T Q\Delta T) \\
&\leq \frac{\sigma_{max}(\widehat{T}_{N,N})\sigma_{max}(Q)\sigma_{max}\Delta T}{\sigma_{min}(\widehat{T}_{N,N}^T Q\widehat{T}_{N,N} + R)} \\
&\leq \frac{(\sigma_{max}(T) + \sigma_{max}(\Delta T))\sigma_{max}(Q)\sigma_{max}(\Delta T)}{\sigma_{min}(R)}
\end{aligned} \tag{3.40}$$

and it can be shown that, if

$$\sigma_{max}(\Delta T) < \frac{-\sigma_{max}(T)}{2} + \frac{1}{2}\sqrt{\sigma_{max}(T)^2 + 4\frac{\sigma_{min}(R)}{\sigma_{max}(Q)}} \tag{3.41}$$

then $sprad(\widehat{K}_{N,N}\Delta T) < 1$. The matrix Q consists of weights on the parameters to be reduced (such as vibration or noise levels) while the matrix R consists of weights on the control inputs (such as flap deflections). If $(\sigma_{min}(R))/(\sigma_{max}(Q))$ is large (minimum energy control), then HHC control possesses a high degree of robustness and a sufficient condition for the stability of HHC algorithm is approximately given by:

$$\sigma_{max}(\Delta T) < \sqrt{\frac{\sigma_{min}(R)}{\sigma_{max}(Q)}} \tag{3.42}$$

However, if $\frac{\sigma_{min}(R)}{\sigma_{max}(Q)}$ is small, the robustness is somehow compromised.

The explicit stability condition in equation (3.42) lends insight into the behavior of the algorithm. This analysis shows that the stability of the algorithm depends on the degree to which $T_{N,N}$ is correctly estimated, or the choice of control weights Q and R. Since the cost function J has not been yet considered, it can be said that even if the algorithm is stable, the estimate of T could affect the attainable minimum. Thus is, a convergence analysis is required. Consider equation (3.35), which can be extended to show

$$\widehat{A}^k = \begin{bmatrix} I_{2p} & T_{N,N} \\ 0 & I_{2m} \end{bmatrix} \begin{bmatrix} I & 0 \\ -\sum_{i=1}^{k-1}(\widehat{K}_{N,N}\Delta T_{N,N})^i \widehat{K}_{N,N} & (\widehat{K}_{N,N}\Delta T_{N,N})^k \end{bmatrix} \begin{bmatrix} I_{2p} & -T_{N,N} \\ 0 & I_{2m} \end{bmatrix} \tag{3.43}$$

Now it is assumed that HHC is stable, that is, equation (3.37) is satisfied. In this case,

$$\lim_{k\to\infty}(\widehat{K}_{N,N}\Delta T_{N,N})^k = 0 \tag{3.44}$$

and one can define a matrix Γ_s such that

$$\Gamma_s = \lim_{k\to\infty}\sum_{i=1}^{k-1}(\widehat{K}_{N,N}\Delta T_{N,N})^i = (I - \widehat{K}_{N,N}\Delta T_{N,N})^{-1} \tag{3.45}$$

Hence equations (3.43), (3.44) and (3.45) imply that

$$\lim_{k\to\infty}\widehat{A}^k = \begin{bmatrix} I - T_{N,N}\Gamma_s\widehat{K}_{N,N} & T_{N,N}(\Gamma_s\widehat{K}_{N,N}T_{N,N} - I) \\ -\Gamma_s\widehat{K}_{N,N} & \Gamma_s\widehat{K}_{N,N}T_{N,N} \end{bmatrix} \tag{3.46}$$

the limiting values of y_k and $\hat{u}_k$ are given by

$$\lim_{k\to\infty}\begin{bmatrix} y_k \\ \widehat{u}_k \end{bmatrix} = \lim_{k\to\infty}\widehat{A}^k\begin{bmatrix} y_0 \\ \widehat{u}_0 \end{bmatrix} = \begin{bmatrix} (I - T_{N,N}\Gamma_s\widehat{K}_{N,N})(y_0 - T\widehat{u}_0) \\ -\Gamma_s\widehat{K}_{N,N}(y_0 - T\widehat{u}_0) \end{bmatrix} \tag{3.47}$$

Next, defining the limiting cost

$$J_{\widehat{T},\infty} = \lim_{k\to\infty}(y_k, \widehat{u}_k \tag{3.48}$$

Substituting equation (3.47) into equation (3.7) yields

$$J_{\widehat{T},\infty} = (y_0 - T\widehat{u}_0)^T\left[Q - QT_{N,N}\Gamma_s\widehat{K}_{N,N} - (QT_{N,N}\Gamma_s\widehat{K}_{N,N})^T + \widehat{K}_{N,N}^T\Gamma_s^T D\Gamma_s\widehat{K}_{N,N}\right](y_0 - T\widehat{u}_0) \tag{3.49}$$

Note that

$$(D^{-1/2}T_{N,N}^T Q - D^{-1/2}\Gamma_s\widehat{K}_{N,N})^T(D^{-1/2}T_{N,N}^T Q - D^{-1/2}\Gamma_s\widehat{K}_{N,N}) \geq 0 \tag{3.50}$$

and hence

$$QT_{N,N}D^{-1}T_{N,N}^T Q \geq QT_{N,N}\Gamma_s\widehat{K}_{N,N} + (QT_{N,N}\Gamma_s\widehat{K}_{N,N})^T - \widehat{K}_{N,N}^T\Gamma_s^T D\Gamma_s\widehat{K}_{N,N} \tag{3.51}$$

Assuming $\widehat{u}_0 = u_0$, equations (3.49), (3.51) and equation (3.17) yield

$$J_{\widehat{T},\infty} \geq J(y, u_{k,opt}) \tag{3.52}$$

which confirms the expected fact that the performance is not better than the optimal performance obtained when T is exactly known.

Now, consider the case where the estimated value $\widehat{T}_{N,N}$ of $T_{N,N}$ involves a multiplicative error, that is

$$\widehat{T}_{N,N} = T_{N,N}(I + \Delta T_{mul}) \tag{3.53}$$

where ΔT is a $2m \times 2m$ matrix. Then $\widehat{T}_{N,N}$ can be expressed equivalently by $\widehat{T}_{N,N} = T_{N,N} + \Delta T_{N,N}$ where

$$\Delta T_{N,N} = T_{N,N} \Delta T_{mul} \tag{3.54}$$

A sufficient condition for stability of HHC is

$$\rho_s(\widehat{K}_{N,N} T_{N,N} \Delta T_{mul}) < 1 \tag{3.55}$$

Substituting equation (3.54) into equation (3.40) yields

$$\rho_s(\widehat{K}_{N,N} T_{N,N} \Delta T_{mul}) = \rho_s((\widehat{T}_{N,N}^T Q \widehat{T}_{N,N} + R)^{-1} \widehat{T}_{N,N}^T Q T_{N,N} \Delta T_{mul}) \tag{3.56}$$

$$\leq \frac{\sigma_{max}^2(T_{N,N}) \sigma_{max}(Q) \sigma_{max}(\Delta T_{mul})(\sigma_{max}(\Delta T_{mul} + 1))}{\sigma_{min}(R)} \tag{3.57}$$

Finally, it can be shown that the algorithm is stable if

$$\sigma_{max}(\Delta T_{mul}) < -\frac{1}{2} + \frac{1}{2}\sqrt{1 + \frac{4\sigma_{min}(R)}{\sigma_{max}^2(T_{N,N})\sigma_{max}(Q)}} \tag{3.58}$$

Anyway, though such an analysis is of course informative, its main limitation lies in the difficulty in relating back bounds on the uncertainty on matrix $T_{N,N}$ to the actual model uncertainty in the dynamics of the helicopter. Based in these considerations, a robust framework could be used to design a control law by incorporating all the uncertainties during the synthesis process.

Conventional HHC deals with the performance degradation in presence of model uncertainties though its adaptive version, which takes into account the variation of matrix $T_{N,N}$ between the different flight conditions. Many different algorithms have been developed in this sense in the last few years, algorithms mainly based on the $T_{N,N}$ estimation at specific time steps during flight operations. In this respect, the interest in investigating a robust control design approach is motivated by the possibility to relax the need for continuous update of the T-matrix.

3.2 Simulations results

In this section, numerical examples are used to illustrate the properties of the algorithm proposed for HHC above described.

3.2.1 Model of the helicopter

The model that will be implemented for control the vibrations of its rotor blade will be the one of the Augusta A109 helicopter, as derived in [4], whose parameters

Table 3.1: Characteristics of the rotor of the Augusta A109 helicopter

Number of blades	4
Rotor angular frequency	40.32 rad/s
Rotor radious	5.5 m
Mass per unit	48.87
Lift curve slope	5.7 rad^{-1}
Lock number	7.8
Blade chord	0.3 m

are the following: The model describes the out-of-plane dynamics of a helicopter rotor blade. Although very simple, this model retains the main characteristics of the full blade dynamics. More precisely, linear out-of-plane bending can be described by the bending equation; to reduce the model to a finite-dimensional representation, a modal expansion for the blade deflection is introduced and truncated to a finite number of nodes. Then, it is possible to show that the partial differential equation is equivalent to a set of ordinary differential equations forced by the aerodynamic load acting on the blade. For the purpose of this work, the pitch angle of the blade is considered as input signal, while the vertical shear force at the root of the blade is the selected output. As discussed in [3], the resulting model can be written as

$$\dot{x}(t) = A(t,\mu)x(t) + B(t,\mu)u(t) \tag{3.59}$$

$$y(t) = C(t,\mu)x(t) + D(t,\mu)u(t) \tag{3.60}$$

where system matrices A, B, C, D are periodic, with period $T = \frac{2\pi}{\Omega}$ functions of time and of the dimensionless advance ratio parameter μ representing the forward speed of the helicopter. The model considered for our purpose is the linear time-invariant by averaging the time periodicity, and choosing $\mu = \bar{\mu} = 0.25$.

3.2.2 Simulation process

The problem described above and the solution designed in the context of the optimal control. In this section have been performed a series of simulations in order to analyse the sensibility and response of the algorithm introduced. The main objective of the following simulations is to identify how the optimal control changes when varying Q and R weights individually. With this purpose, and considering the one-step convergence of the algorithm (see 3.1.2), a time-domain simulation has been carried out. The T matrix used in the algorithm for the simulations is the following:

$$T_{N,N} = \begin{bmatrix} -0.2318 & 0.0252 \\ -0.0252 & -0.2318 \end{bmatrix} \tag{3.61}$$

3.2.3 Results

Sensitivity to Q and R weights

Firstly, the analysis will explore the response of the control to the changes in the weight matrices that penalize the control effort (R) and the transient state deviation (Q). Since the best performance of the controller is reached after the first update, results of the value of the H_2 norm for the different values of the weight are collected and plotted. Moreover, also the values of the H_2 norm of the control input are plotted for a better understanding of its behaviour. With this purpose, being $R = \rho * I$ a sensitivity analysis to R (with $Q = 1 * I$) have been done.

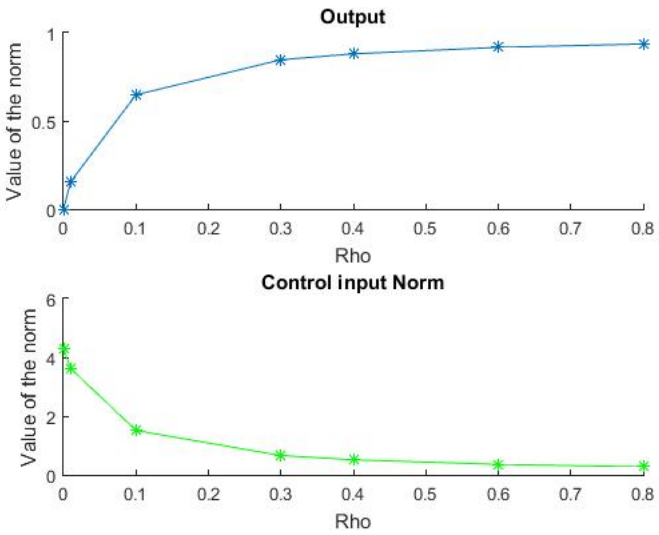

Figure 3.1: Sensitivity to weight matrix R

Analysing figure 3.1, it can be noticed a loss of performances the value of the weight R increases since the control input is being penalized. As expected with null weight imposed to the control input effort, meaning that the control input action can take any value, the optimal performance is reached, giving a full attenuation of the vibration level at the output. In view of the obtained result, it is easy to see that even changing Q, if $R = 0$, the total attenuation is always achieved.

Considering $Q = \alpha * I$ a sensitivity analysis to Q (with $\rho = 0.1$) have been done.

Related to the changes in the Q weight, from figure 3.2, it can be noticed that as alpha increase its value, the performance improve, as expected, since we are penalizing the state deviation. It is the weight applied on the parameter to be reduced, e.g., in the vibration level. Anyway, as pointed before, when R weight is 0, the system is insensitive to changes in Q.

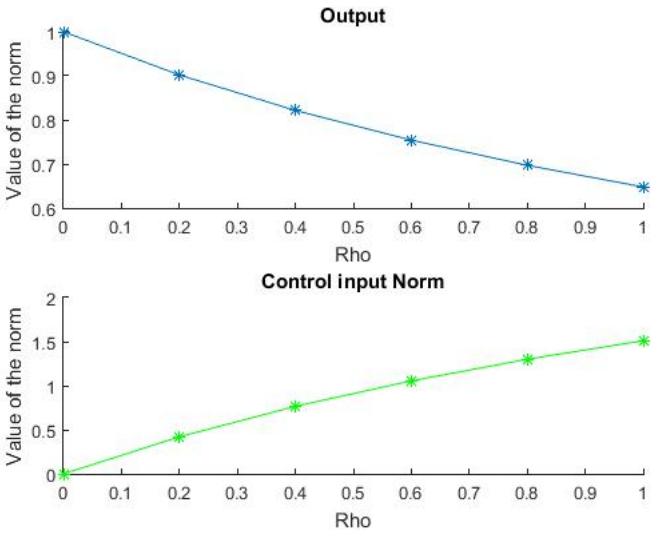

Figure 3.2: Sensitivity to weight matrix Q

Moreover, a LQ simulation with Simulink was performed to evaluate the time response of the system when a sinusoidal disturbance is introduced. The controller was tuned with $R = 0 * I$, $Q = I$. Figure 3.3 shows how the LQ controller is able to attenuate the disturbance completely.

Loss of performance with uncertain T matrix

In this section, simulation results are used to illustrate the loss of performance of the LQ controller when the T-matrix is not known exactly, so, adding uncertainty to the system. In order to get the T-matrix as in (3.5), one can evaluate the frequency of the model, leading to the following the nominal matrix $\bar{T}_{N,N}$

$$\bar{T}_{N,N} = \begin{bmatrix} -0.2318 & 0.0252 \\ -0.0252 & -0.2318 \end{bmatrix} \tag{3.62}$$

The weight parameters are:
$R = 0.1 * I$ $Q = 1 * I$
and the uncertainty in the T-matrix considered as

$$T_{N,N} = \bar{T}_{N,N} + (I + rW\delta), \quad |\delta| < 1 \tag{3.63}$$

where I is the identity matrix, δ is a normalized representation of the uncertainty, r is a scalar scale factor and W represents the uncertainty ellipsoid affecting the frequency response $G(j\omega)$ at the disturbance frequency. So, in this example W is defined in this way, and changing the value of r, three different results are illustrated.

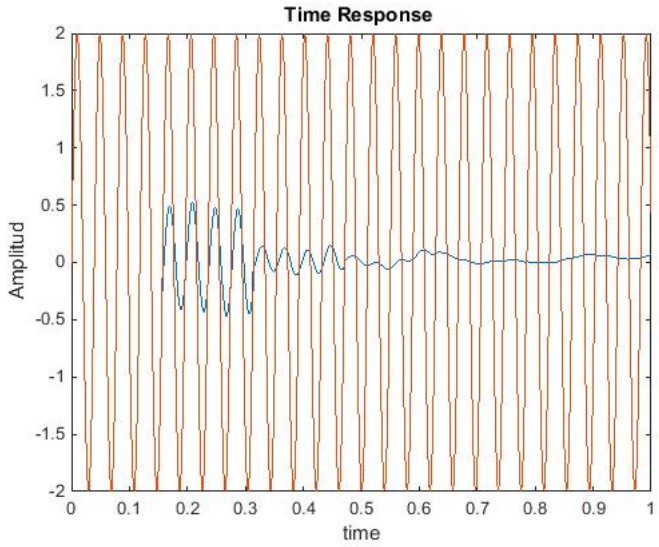

Figure 3.3: LQ controller time response

EXAMPLE 1

$$rW = 0.1 \begin{bmatrix} 1 & 1 \\ -1 & 1 \end{bmatrix} \tag{3.64}$$

δ radomly bearing from 0 to 1. $T = \bar{T}(I + W)$
EXAMPLE 2

$$rW = 0.2 \begin{bmatrix} 1 & 1 \\ -1 & 1 \end{bmatrix} \tag{3.65}$$

δ radomly bearing from 0 to 1. $T = \bar{T}(I + W)$
EXAMPLE 3

$$rW = 0.5 \begin{bmatrix} 1 & 1 \\ -1 & 1 \end{bmatrix} \tag{3.66}$$

δ radomly bearing from 0 to 1. $T = \bar{T}(I + W)$

A comparison between the three examples has been carried and results are collected in Table 3.2, where Mean y refers to the mean value of the H_2 norm at the output, Max y is the maximum value of the norm, deviation y and Ts is the settling time.

As can be appreciated in Table 3.2 the settling time is highly sensitive to variations on the level of uncertainty of the T-matrix. Remark, as expected, the deviation of the results increases when the level of uncertainty grows. Notice that the mean value of the output does not present important variations and remain around 0.6, meaning that a 40% of attenuation has been made.

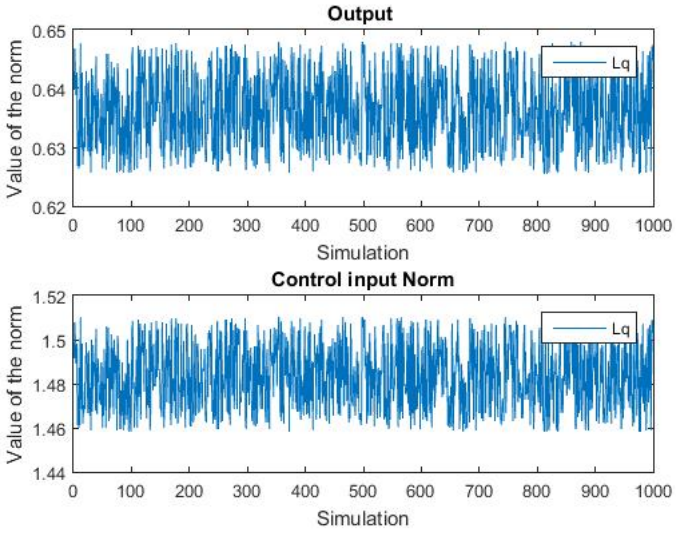

Figure 3.4: Loss of performance when adding uncertainty (Example 1)

Table 3.2: Comparison between different levels of uncertainty on T-matrix

LQ	W=0.1.*[1 1; -1 1]	W=0.2.*[1 1; -1 1]	W=0.5.*[1 1; -1 1]
Mean y	0.63637	0.62504	0.59469
Max y	0.64789	0.64784	0.64788
Deviation y	0.0064866	0.012592	0.030113
Ts (s)	1.905	1.963	2.993

Unstable results with T uncertain

Consider the nominal T-matrix $\bar{T}_{N,N}$ given by

$$\bar{T}_{N,N} = \begin{bmatrix} 1 & 3 \\ -3 & 1 \end{bmatrix} \tag{3.67}$$

and the relative uncertainty

$$rW = 0.48 \begin{bmatrix} 1 & 2 \\ -2 & 1 \end{bmatrix} \tag{3.68}$$

The LQ controller is based on the weights $Q = I$ and $R = 0.1I$. A Monte Carlo study was carried out, by randomly choosing 1000 values for the normalized uncertainty δ. Figure 3.7 reveals the results obtained, where the steady state of the output y_N is shown. Recalling that a unit-norm is affecting the system clearly it is shown that LQ controller is subjected to instability.

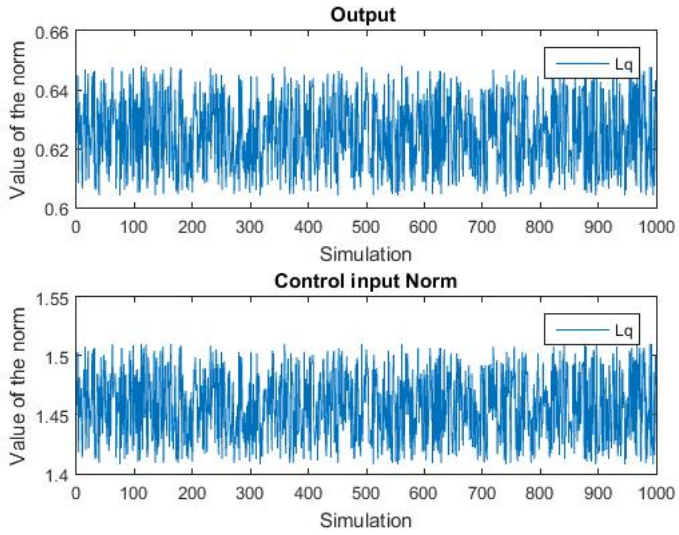

Figure 3.5: Loss of performance when adding uncertainty (Example 2)

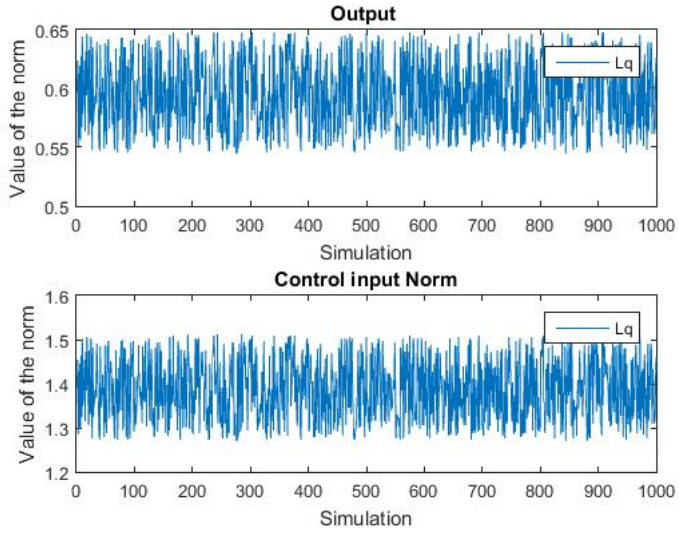

Figure 3.6: Loss of performance when adding uncertainty (Example 3)

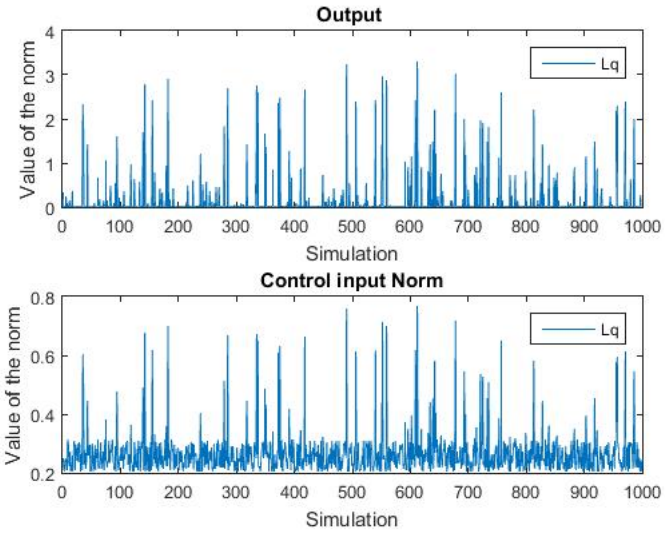

Figure 3.7: Monte Carlo study: steady state magnitude of the output for LQ controller

Chapter 4

Robust control approach: H_∞ controller

4.1 Numerical Analysis

As previous results obtained in Chapter 3 revealed, optimal control presents an important loss of performance when the model of the system is not certain and, in some cases, instability can occur. Therefore, a robust framework could be used to design a control law by incorporating uncertainty.

In the following a robust H_∞ approach to the design of the HHC control law is presented. The multiplicative representation of uncertainty is considered

$$T_{N,N} = T_{N,N}(1 + rW\delta), \quad \delta < 1 \tag{4.1}$$

where I is the identity matrix, δ is a normalized representation of the uncertainty, r is a scalar scale factor and W represents the uncertainty ellipsoid affecting the frequency response $G(j\omega)$ at the disturbance frequency. Notice that matrix W has the same structure as the T-matrix. In figure 4.1, a block diagram represents schematically the uncertain feedback system of the model, its uncertainty and the controller.

With reference to figure 4.1, variables $y_{0,\delta}$ and y_δ can be defined as

$$\begin{aligned} y_\delta(k) &= rW\bar{T}_{N,N}u_N(k) \\ y_{0,\delta}(k) &= \delta y_\delta(k), \end{aligned} \tag{4.2}$$

resulting the uncertain control-loop system

$$\begin{aligned} u_N(k+1) &= K_M u_N(k) + K_N y_N(k) \\ y_N(k) &= \bar{T}_{N,N}u_N(k) + y_{0N} + y_{0,\delta}(k) \\ y_{delta}(k) &= rW\bar{T}_{N,N}u_N(k) \\ y_{0,\delta} &= \delta y_\delta. \end{aligned} \tag{4.3}$$

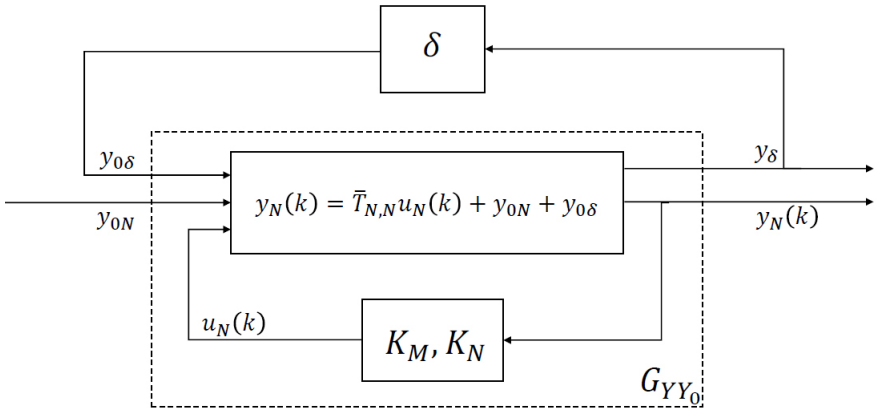

Figure 4.1: Block diagram of the uncertain feedback system

Letting $Y = [y \quad y_\delta]^T$ and $Y = [y_{0N} \quad y_{0,\delta}]^T$ the previous system takes the form:

$$Y = GT_{Y,Y_0}(z)Y_0 \tag{4.4}$$

To complete the formulation of the H_∞ synthesis problem, the weighting functions W_z and W_u are defined, respectively, on the output y_N and on the control variable u_N according to the block diagram for the augmented plant model in Figure 4.2 In particular, the frequency response of $W_z(z)$ can be designed keeping in mind

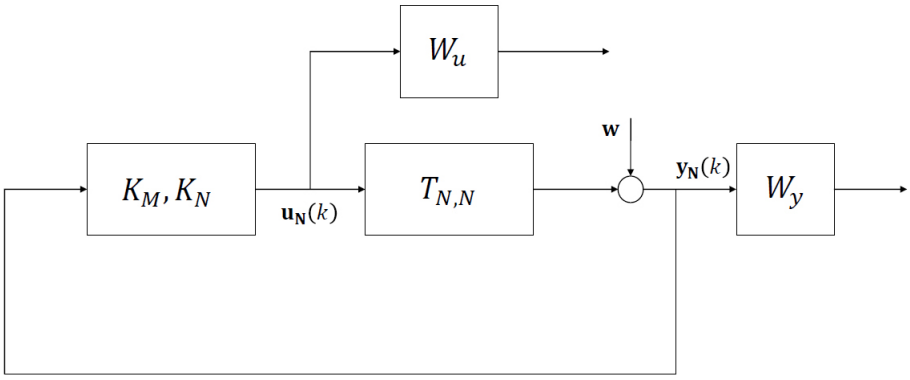

Figure 4.2: Augmented plant model[Mura]

that the goal is the vibration reduction at steady-state. Consequently, the robust synthesis problem can be formulated as where G_{uy_0} is the control sensitivity function, obtained by re-opening the closed-loop from the disturbance y_{0N} to the control variable u_N in the nominal case

$$G_{yy0} = (zI - (K_M + K_N\bar{T}_{N,N}))^{-1}K_N \tag{4.6}$$

$$\begin{aligned} &\text{Find} \quad K_M, \quad K_N \\ &\text{s.t} \end{aligned}$$

$$\left\| \begin{matrix} G_{YY_0} W_y \\ G_{uy_0} W_u \end{matrix} \right\|_\infty \leq \gamma \tag{4.5}$$

4.2 Simulation results

4.2.1 Simulation process

The problem presented (4.5) is a structured H_∞ problem, which is known to be both non-convex, so that the convergence of the algorithm may depend on the initial controller and global optimality of the computed solution cannot be guaranteed, and non-smooth, that is gradient-based descent algorithms could fail. Tanking it in consideration, a stochastic process can be used to solve the optimization problem: it should be noticed that the control law is considered optimal if in its neighborhood a better control law cannot be found or can be found with null probability.

In view of this, assume that an initial stabilizing controller, based on the LQ T-matrix algorithm, is available. To compute a new controller $K^{(i+1)}$ the simulations have been done using as a minimization procedure the fminsearch function given by MATLAB software were the termination criterion is set to a tolerance of 10^{-4}. The fminsearch is a direct search method that does not work using numerical or analytic gradients. A 3-simplex (triangle) is characterized since the problem is defined in two-space, in such manner, at each step, a new point is created in or near the simplex. The function achieved in that point is compared with the one of the vertices of the simplex, and, the new point replaces one of those vertices. This is continuously repeating until the diameter of the simplex is less than the indicated tolerance.

The gains of the LQ T matrix are not fully parametrized 2×2 matrices but inherit the structure of the T matrix itself. This structure of the control law can be either maintained in the design of the robust controller, or , contrarily, can be relaxed leading to a fully parametrized control law. Consequently a comparison of both controllers have been performed.

In figures 4.3 and 4.4 can be seen how the structure on the controller affects the minimizations procedure. Considering an initial LQ controller with the given weights $Q = I$,$R = 0$ and the nominal T-Matrix $T_{N,N}$:

$$T_{N,N} = \begin{bmatrix} -0.2318 & 0.0252 \\ -0.0252 & -0.2318 \end{bmatrix} \tag{4.7}$$

(Note that no weight on the control action has been included). The results showed that a fully parametrized structure is able to achieve greater minimization of the

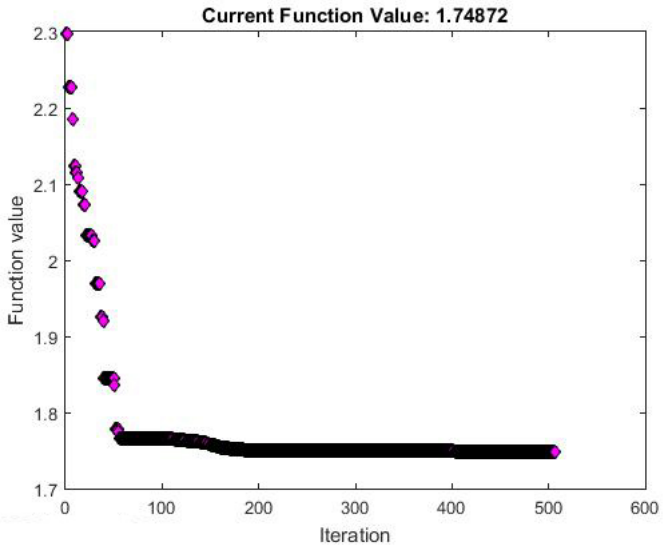

Figure 4.3: Cost function value with a Unstructured H_∞ Controller

cost function since all entries of the matrices M and N can be set independently. Instead structured M, N matrices present less possibilities of variations since the values of the diagonal and off diagonal are constrained to maintain the same structure as the T matrix. Therefore the structure represents a limitation in terms of cost function minimization although the difference it is not significant.

However the stopping criterion is achieved faster in the case of a structured controller rather than the unstructured one.The behaviour presented is justified since the number of parameters to be set in the optimization procedure are less in case of a structured controller and therefore number of possibilities to which the minimization procedure has to go through.

This behaviour becomes interesting when the tuning velocity of the controller is more important over the globality of the minimum solution of the problem 4.5

Consider the nominal T-Matrix $T_{N,N}$ given by

$$T_{N,N} = \begin{bmatrix} -0.2318 & 0.0252 \\ -0.0252 & -0.2318 \end{bmatrix}$$

and the relative uncertainty

$$rW = 0.2 \begin{bmatrix} 1 & 1 \\ -1 & 1 \end{bmatrix}$$

For this system unstructured and structured H_∞ controllers have been designed.Several simulations have been performed in order to test the sensitivity to variations on the steady-state reference attenuation.Where the weighting function is given by

$$W_z(s) = \frac{s + eps * 40}{s/0.99 + 40}$$

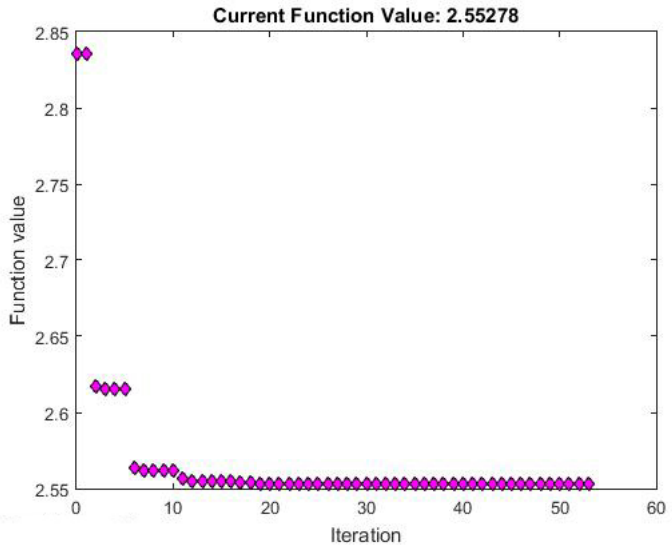

Figure 4.4: Cost function value with a structured H_∞ Controller

(no weight on the control action has been included).Parameter *eps* represents the steady-state reference attenuation.

As noticed in figure 4.5 (a) and figure 4.6 (a) structured and non structured controllers are achieving the attenuations levels imposed by the weighting function in most of the cases. Nevertheless this situation changes significantly when weight on the control action is included since the control action is limited. See figure 4.5 (b) and figure 4.6 (b) where the following weight have been applied

$$W_u(s) = \frac{0.01s + 200}{s + 400}$$

By including the control weight the control input has been limited significantly and therefore the output achieved in all situations is far from the objective. On view of this results, the choice of the actuators acting on the system it is not trivial and it has great influence on the performance of the control system. Therefore the actuators have to be chosen taking into account energy consumption, weight and also the limitation they create into the control system.

Other simulations have been performed to study the sensitivity to the ratio Q/R . In this simulations H_∞ structured controller presented lack of sensibility to this ratio(Figure 4.7 (a))due to the fact that the same structure of the T matrix is held. Instead unstructured H_∞ controller (Figure 4.7 (b))presented a behaviour more sensitive to the ratio Q and R which is more interesting for a real MIMO problem enabling the possibility to define different targets depending on which part of the fuselage is wanted to be attenuated.

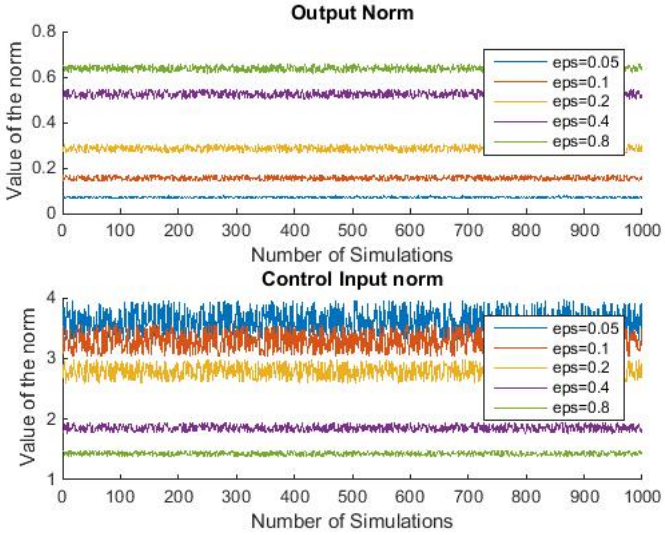

(a) No weighted Control action

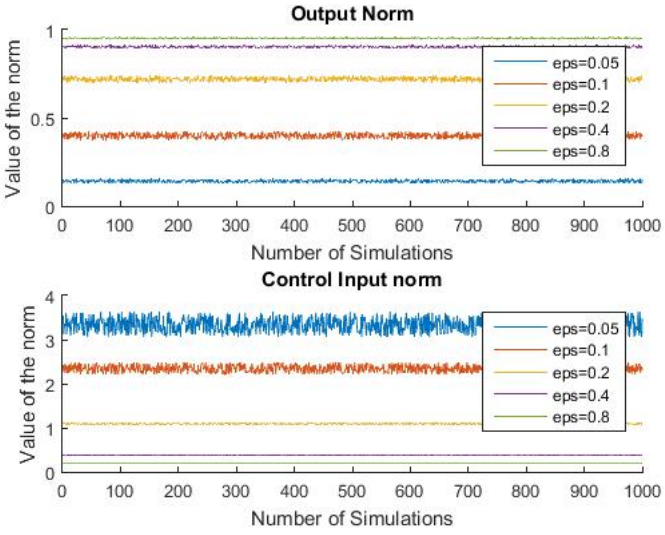

(b) Weighted Control action

Figure 4.5: Unstructured H_∞ Controller eps sensitivity

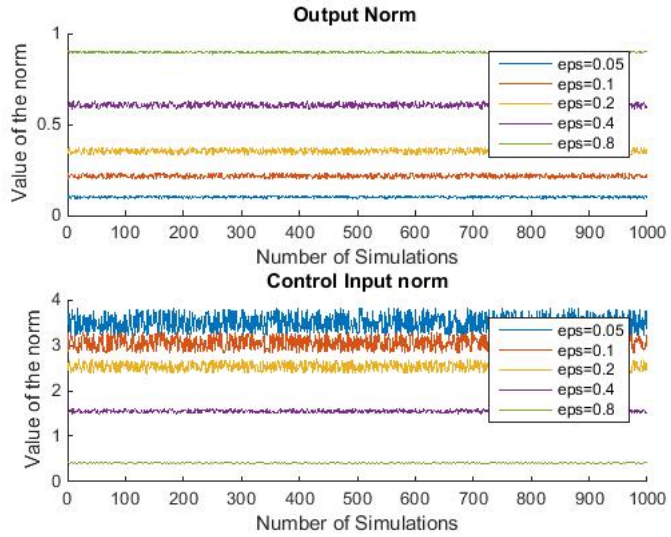

(a) No weighted Control action

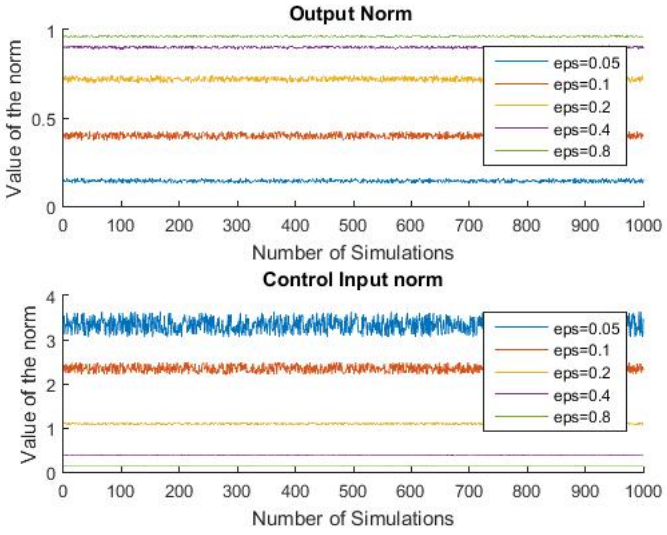

(b) Weighted Control action

Figure 4.6: Structured H_∞ Controller eps sensitivity

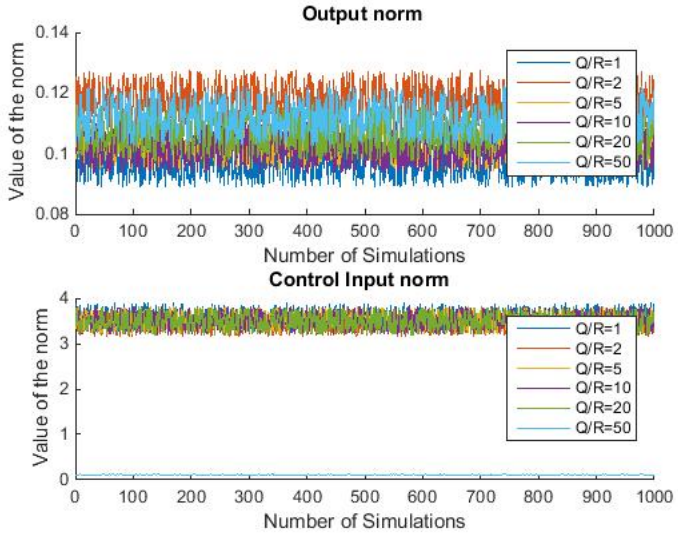

(a) Structured H_∞ Controller

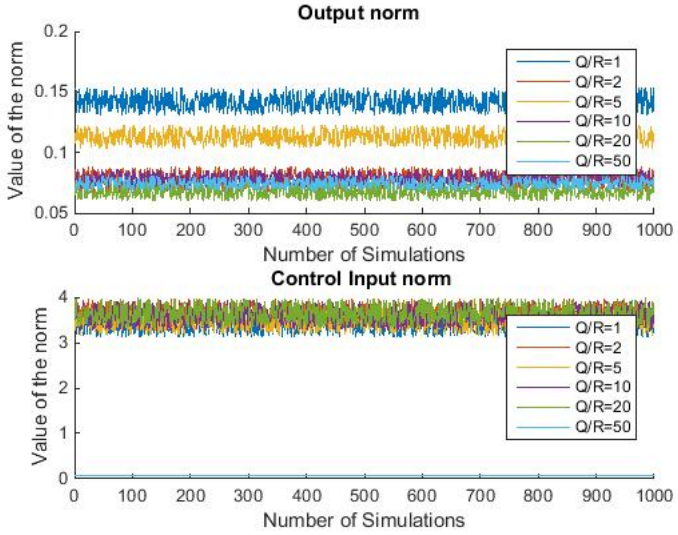

(b) Unstructured H_∞ Controller

Figure 4.7: Q/R sensitivity

Chapter 5

Conclusion

Hovering and vertical take off are abilities that make helicopters irreplaceable aircrafts. But the unsteady rotor flow in forward flight as well as the interaction of rotor vortices creates noise and vibrations that reduces the level of comfort and increase the costs and maintenance efforts. In view of that different controllers have been designed in order to reduce noise and vibrations.

An optimal control based on a LQ controller have been designed and revealed a possible minimization through the T matrix algorithm. Nevertheless the loss of performance and instability when the model of system presents uncertainty makes the robust control a more reliable solution.

Different robust solutions can be implemented to overcome this problem. A structured controller (same structure as the T matrix) or an unstructured controller. The results showed that an structured controller is interesting since it is able to achieve similar attenuations levels as the unstructured controller but with favourable property of tuning the controller quicker. Instead the unstructured controller presents more interesting properties for the capability of different targeting as simulations revealed.

Bibliography

[1] Mark Achache and Michel Polychroniadis. Development of an experimental system for active control of vibrations of helicopters–development methodology for an airborne system. *VERTICA.*, 11(1):123–138, 1987.

[2] Peter J Arcidiacono. Theoretical performance of helicopters having second and higher harmonic feathering control. *Journal of the American Helicopter Society*, 6(2):8–19, 1961.

[3] Sergio Bittanti and Marco Lovera. On the zero dynamics of helicopter rotor loads. *European Journal of Control*, 2(1):57–68, 1996.

[4] W Johnson. Helicopter theory, 1980.

[5] Ch Kessler. Active rotor control for helicopters: individual blade control and swashplateless rotor designs. *CEAS Aeronautical Journal*, 1(1-4):23–54, 2011.

[6] Ch Kessler. Active rotor control for helicopters: motivation and survey on higher harmonic control. *CEAS Aeronautical Journal*, 1(1-4):3–22, 2011.

[7] Roberto Mura, Amir Masoud Ghalamzan Esfahani, and Marco Lovera. Robust harmonic control for helicopter vibration attenuation. In *American Control Conference (ACC), 2014*, pages 3850–3855. IEEE, 2014.

[8] Roberto Mura and Marco Lovera. Baseline vibration attenuation in helicopters: robust mimo-hhc control. *Proc. 19th World Congr., Int. Fed. Autom. Control*, pages 8855–8860, 2014.

[9] Daniel Patt, Li Liu, Jaganath Chandrasekar, DS Bernstein, and PP Friedmann. The hhc algorithm for helicopter vibration reduction revisited. In *Proceedings of the 45 th AIAA/ASME/cE/AHS/ACS Structures, Structural Dynamics and Materials Conference, Palm Springs, CA, April 2004. AIAA Paper No. 2004-1948*, 2004.

[10] John T Pearson and Roger M Goodall. Adaptive schemes for the active control of helicopter structural response. *Control Systems Technology, IEEE Transactions on*, 2(2):61–72, 1994.

[11] JT Pearson, RM Goodall, and I Lyndon. Active control of helicopter vibration. *Computing & Control Engineering Journal*, 5(6):277–284, 1994.

[12] Peter Richter, Hans-Dieter Eisbrecher, and Valentin Klöppel. *Design and first tests of individual blade control actuators*. Messerschmitt-Bölkow-Blohm, 1990.

[13] John Shaw and Nicholas Albion. Active control of the helicopter rotor for vibration reduction. *Journal of the American Helicopter Society*, 26(3):32–39, 1981.

[14] E Roberts Wood, Richard W Powers, John H Cline, and C Eugene Hammond. On developing and flight testing a higher harmonic control system. *Journal of the American Helicopter Society*, 30(1):3–20, 1985.

[15] ER Wood, RW Powers, and CE Hammond. On methods for application of harmonic control. *Vertica*, 4(1):43–60, 1980.

List of Figures

List of Tables